Title

Sol-gel coatings for metallic prosthesis from methyl-modified alkoxysilanes: balance between protection and bioactivation

Authors

F. Romero-Gavilán[1*], J. Carlos-Almeida[2], A. Cerqueira[1], M. Gurruchaga[3], I. Goñi[3], I. M. Miranda-Salvado[2], M.H. Vaz Fernandes[2], J. Suay[1]

[1] Departamento de Ingeniería de Sistemas Industriales y Diseño. Universitat Jaume I, Av. Vicent-Sos Baynat s/n. Castellón 12071. Spain.

[2] CICECO – Aveiro Institute of Materials, Department of Materials and Ceramic Engineering. University of Aveiro, 3810-193 Aveiro. Portugal.

[3] Facultad de Ciencias Químicas. Universidad del País Vasco. P. M. de Lardizábal, 3. San Sebastián 20018. Spain.

[*]Corresponding author: Francisco Romero-Gavilán

Abstract

The osteogenic properties displayed by hybrid silica sol-gel materials make these compositions perfect candidates to be employed in bone tissue engineering applications. The present study aims to develop and characterize hybrid silica coatings, synthetized from mixtures between tetraethyl-orthosilicate (TEOS) and three different methyl-modified alkoxysilanes: trimethoxymethylsilane (MTMS), dimethyldiethoxylsilane (DMDES) and polydimethylsiloxane (PDMS). The comparison of the properties of these materials would allow to determinate which one is the best option to be applied onto metallic prosthesis for bone tissue application. After optimizing the synthesis parameters, the developed coatings were characterized using Fourier transform infrared spectrometry (FT-IR), ^{1}H and ^{29}Si solid state Nuclear Magnetic Resonance (^{1}H-NMR and ^{29}Si-MNR), cross-cut tests, contact angle measurements, optical profilometry, hydrolytic degradation tests and electrochemical impedance spectroscopy essays (EIS). Homogeneous and well-adhered coatings were obtained with the three methyl-modified reagents. However, different behaviours of metal protection against corrosion, hydrophilicity and degradation kinetics resulted depending on the initial precursor. The MTMS-based coating showed the highest hydrophilicity and degradation kinetics, properties that can lead to a greater bioactivity (Si release). While PDMS and DMDES-based coatings presented a higher barrier properties. From the physicochemical standpoint, all these materials presented interesting characteristics to be employed as coatings for biomedical applications.

Keywords:

Hybrid sol-gel; biomaterials; alkoxysilane; metal prosthesis; corrosion resistance; coating

1. Introduction

In 1969, Larry Hench found that certain glass compositions of the $Na_2O–CaO–P_2O_5–SiO_2$ system were able to form a strong and stable bond to bone [1]. Following this first bioglass, novel silica materials with improved features such as hybrid sol-gel compounds have appeared providing new possibilities in the tissue engineering field [2].

The sol-gel route is a versatile technique to design materials, which makes possible to synthetize networks with different properties in terms of hydrophilicity, morphology, porosity, chemistry or degradability by controlling reaction parameters such as precursor nature, temperature, pH, H_2O:Si ratio and type of solvent [3]. In addition, the use of organically modified alkoxysilanes allows the incorporation of organic functional groups in the network giving rise to hybrid compounds [4].

Silicon is an essential element for bone metabolism; in fact, its significant effect on early stages of bone formation has been known for a long time [5]. Silicon hybrid networks are biocompatible and biodegradable, being able to release $Si(OH)_4$. This compound is related to the promotion of type I collagen synthesis and osteoblastogenesis, favouring bone regeneration [6]. As a consequence, silica hybrid materials display a great potential for hard tissue biomedical applications [7].

The sol-gel technique allows to apply these networks as coatings, reaching a strong adhesion to the substrate. As a result, their use onto metallic prosthesis, such as dental implants, hip replacements, intramedullary nails or osteosynthesis plates and their screws, is an interesting application [8]. Not only the prosthesis bioactivation, by the release of Si compounds, can be achieved with an improved implant capability to bond to the host bone, but also these coating can perform protective functions to the metallic substrates [9]. This behaviour may be especially relevant to prevent corrosion phenomena and the migration of their products, which could lead to the prosthesis rejection [10].

The siloxane precursor trimethoxymethylsilane (MTMS), which has a methyl as a functional group, is employed to develop sol-gel treatments on metallic prosthesis. Martínez-Ibáñez *et al.* [11] studied sol-gel networks based on combinations of MTMS and tetraethyl orthosilicate (TEOS) in different proportions. These MTMS:TEOS sol-gel networks were applied as coating onto titanium dental implants and it was found that the ratio 7:3 could achieve an earlier new bone growth *in vivo* in comparison to the uncoated Ti. Similarly, triple combinations of MTMS, 3-glycidoxypropyl-trimethoxysilane (GPTMS) and TEOS alkoxisilanes were designed and applied as coatings onto AISI 316L stainless steel [9]. This study revealed that an optimal balance between the release of Si and the prosthesis protection could be achieved by modifying the percentage of TEOS. The dimethyldiethoxylsilane (DMDES) precursor allows to incorporate twin methyl groups on the sol-gel structure. Different researchers have investigated the sol-gel reactions related to the DMDES:TEOS network formation [12,13]. DMDES:TEOS organically modified silicates were successfully applied as a coating onto silica substrates for optical applications [14]. Nevertheless, there is a limited number of studies focused on the use of DMDES-derived materials for biomedical applications [15,16], being these sol-gel networks employed as a monolith and not as a coating for metallic prosthesis. Sol-gel coatings with anticorrosive properties for biomedical application were also developed using polydimethylsiloxane (PDMS), DMDES polymerized chains, and TEOS as precursors [17]. In addition, PDMS-derived coatings proved to be non-cytotoxic [18–20].

In this work, we developed and characterized methyl modified silica coatings onto AISI 316 stainless steel, synthetized in the same conditions, from TEOS and three different organically-modified alkoxysilanes (MTMS, DMDES and PDMS). We aimed to study how the initial precursor selection affected the final sol-gel material properties in order to determine which compound was the best option to design coatings for tissue engineering applications.

2. Materials and methods

2.1. Sol-gel synthesis and sample preparation

Three distinct compositions were synthetized through the sol-gel route. The corresponding methyl-modified precursor MTMS ($CH_3Si(OCH_3)_3$), DMDES ($(CH_3)_2Si(OC_2H_5)_2$) or silanol terminated PDMS ($HO[-Si(CH_3)_2O-]_nH$; 550 g mol^{-1} average molecular weight) were mixed with TEOS in a molar ratio 1:3. The nomenclature used in the study is shown in Table 1. All these reagents were purchased from Sigma-Aldrich (St. Louis, MO, USA).

The selection of the molar ratio 1:3 between the alkoxysilanes was based on the limitation found for obtaining samples with the PDMS:TEOS combination, as it was not possible to produce proper coatings with higher amounts of PDMS. Considering that PDMS molecule is a polymerized chain of DMDES, an additional composition with 4 % PDMS and 96 % TEOS, was synthesized as control to achieve a deeper understanding of structural and chemical differences between DMDES and PDMS precursors maintaining a constant number of organically-modified silicon atoms. For this reason, this composition was only chemically characterized.

2-propanol (Honeywell Fluka TM, New Jersey, US) was used as solvent with a volume ratio alcohol:siloxane 1:1. Afterwards, the necessary stoichiometric amount of water to carry out the precursor hydrolysis was added at a 1 drop s^{-1} rate. This reaction was carried out under acid catalysis conditions, for which the added water was previously acidified with 0.1 M HCl (Panreac, Barcelona, Spain). The mixtures were stirred for 1 h and then were kept at rest for 2 h at room temperature. After this time, samples were immediately prepared using the obtained sol-gel solutions.

Table 1. Molar percentage of the developed hybrid sol-gel materials.

Reference	MTMS (%)	DMDES (%)	PDMS (%)	TEOS (%)
25M:75T	25	-	-	75
25D:75T	-	25	-	75
4P:96T	-	-	4	96
25P:75T	-	-	25	75

Finally, the obtained materials were cured through a heat treatment, which consists in keeping the samples in an oven at 60 ºC for a week and then the samples were heated at 120 ºC for 24 h.

2.2. Sample preparation

Three different types of samples were prepared, following the requirements of the distinct characterization methods:

To obtain monolithic samples the sol-gel mixtures were poured into 55 mm diameter polypropylene petri dishes and then were cured under the conditions described in 2.1 at 60ºC. After that, the monoliths were put in glass petri dishes to be heated until 120 ºC.

To prepare coatings, AISI 316-L stainless steel plates (5 cm x 5 cm; RNSinox S.L., Spain) were used as substrates. The stainless steel surfaces were pre-treated by polishing and then cleaned with acetone to remove impurities. The film deposition was performed employing a dip-coater (KSV instrument-KSV DC). Substrates were immersed into the sol-gel solutions at a speed of 60 cm min^{-1}, kept immersed for one minute, and finally they were removed at a 100 cm min^{-1} speed.

Coatings were also prepared onto glass slides using flow-coating technique. These glass surfaces were previously cleaned in an ultrasonic bath (Sonoplus HD 3200) for 20 min at 30 W with nitric acid

solution at 25 % volume. An additional cleaning was carried out with distilled water under the same conditions. Then, the slides were dried at 100 °C.

2.3. Physico-chemical characterization

Fourier Transform Infrared Spectrometry (FT-IR) and solid state Nuclear Magnetic Resonance (NMR) were employed to structurally and chemically characterize the developed hybrid networks. For that, the monolith samples were crushed in a mortar to create fine powders.

Pellets of each composition were made using spectroscopic grade dried KBr powder in order to perform the FT-IR analysis. The spectra were recorded in the 350 - 4000 cm^{-1} wavelength range with a 4 cm^{-1} resolution using a spectrometer model Mattson 7000 (Mattson-Garvin, Texas, US). Solid-state NMR spectroscopy was used to evaluate the crosslinking density of the silicon network. The spectra were obtained using a Bruker 400 AVANCE spectrometer, equipped with a Cross Polarization Magic Angle Spinning (CP-MAS) probe (Bruker, Billerica, US). ^{1}H MAS-NMR measurements were carried out at 12 and 15 KHz sample rotation speed, using a probe of 4 mm, a 3 µs pulse width and a delay time of 5 s. For ^{29}Si MAS-NMR the sample rotation speed was 5.0 kHz, the pulse width was 4.5 µs and the delay time was 60 s, using a probe of 7 mm. The measurements were performed operating at a 79.5 MHz frequency. Kaolinite was used as the chemical shift reference.

The adhesion of the sol-gel coatings onto the stainless steel plates was evaluated by the cross-cut test (UNE EN-ISO 2409:2013). A mechanical Dektak 6 M profilometer (Veeco, Plainview, NY, USA) was used to characterize the roughness and the thickness of the coatings. Two samples of each sol-gel material were tested, with three measurements for each sample. The roughness was determined using their arithmetic average parameter (Ra). Contact angle measurements were performed to determine the sol-gel coating wettability using an optical contact angle meter SL200HT (USA KINO Industry Co., Shanghai, China). Volumes of 10 µL of distilled water were deposited on the coated

stainless steel samples at room temperature, taking the images after 20 seconds from the drop formation. 15 drops were deposited on each sample and a total of three samples identically prepared of each composition were analyzed. The contact angles were measured from the obtained drop images by image processing using ImageJ software with Contact Angle plug-in (https://imagej.nih.gov/ij/).

The hydrolytic degradation of the sol-gel coatings was evaluated using the flow coated glass slides. The degradation kinetics was determined through the measured mass loss, weighting the samples before and after soaking in 100 mL distilled water at 37 ºC for periods of 7, 28, 52 and 84 days. The samples were dried in a vacuum oven at 37 ºC for 48 h before and after soaking. Each data point is the mean of three measurements performed in three different samples identically prepared.

EIS measurements were performed on the sol-gel films deposited on the stainless steel substrates at different exposure times to 3.5 % wt NaCl in deionized water for up to 48 h in order to evaluate their corrosion protection capability. Measurements were carried out after 0, 1.5, 3, 4, 6, 8, 10, 24 and 48 h of exposure to this solution with a test surface area of 3.14 cm^2 in all cases. The assays were carried out using an Impedance Measurement Unit IM6 (Zahner-elektrik, Kronach, Germany). A three-electrode electrochemical cell was employed, where the sample without coating acted as the working electrode, an Ag/AgCl electrode was used as reference and a graphite sheet was employed as counter-electrode. The free corrosion potential mode was used to conduct the tests. A frequency range from 10 mHz to 100 kHz with a sinusoidal voltage perturbation of 10 mV amplitude was applied to the system. All tests were performed in a Faraday cage. Each material was tested at least three times in order to check reproducibility. Two equal results are considered valid and the results shown are from the most representative sample.

3. Results

3.1. FT-IR analysis

The sol-gel materials from distinct methyl-modified alkoxysilanes were chemically characterized using FT-IR. The obtained spectra are shown in Figure 1. All samples present infrared bands in the 370-3500 cm^{-1} region. Bands at 560 cm^{-1}, 807 cm^{-1} and 1070 cm^{-1} were attributed to the Si-O-Si bond vibrations in siloxane rings, symmetric stretching and asymmetric stretching modes, respectively [21,22]. Bands at 435 and 850 cm^{-1} are related to the presence of hybrid cross-linked Q units (TEOS) – D units (DMDES and PDMS) structures in 4P:96T, 25P:75T and 25D:75T samples [23]. These bands also appear in the 25M:75T, but in this case signal at 850 cm^{-1} is shifted to 830 cm^{-1}, and are likely associated to the formation of Q-T structures. The presence of methyl groups in the siloxane networks was confirmed by the detection of its characteristic band at 1270 cm^{-1} [24]. In addition the bands at 2925 and 2980 cm^{-1}, can be assigned to asymmetrical and symmetrical C-H stretching in CH_3, respectively [25]. The shoulder around 3450 cm^{-1} can be connected to the vibration of hydroxyl species, and the band at 1635 cm^{-1} is related to the vibration of O-H bond in H_2O [23,24]. Additionally, Si-OH band was detected at 950 cm^{-1} in 4P:96T, 25D:75T and 25M:75T networks [23].

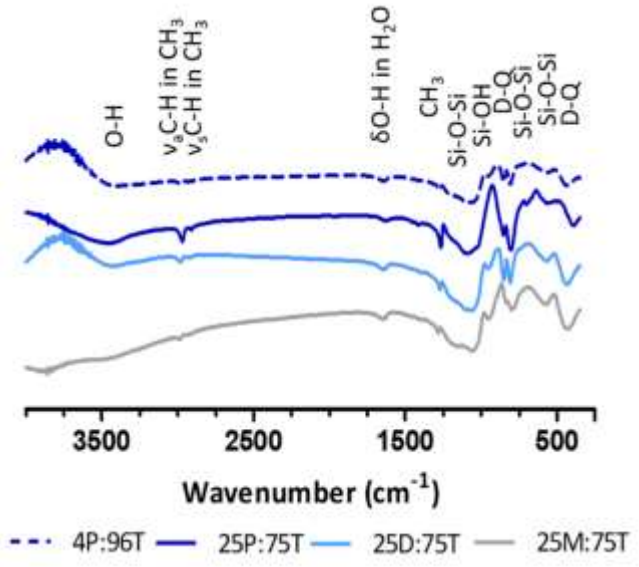

Figure 1. FT-IR spectra of hybrids synthetized using different precursors.

3.2. Solid-state ^{1}H MAS and ^{29}Si MAS NMR analysis

The obtained sol-gel network structures were analysed by ^{1}H MAS and ^{29}Si MAS NMR. Figure 2 shows the ^{1}H MAS NMR spectra. The peak detected between 0.07 and 0.20 ppm, depending on the network, is related to the CH_3 groups incorporated into the structure by the distinct alkoxysilanes [26]. A more intense signal was detected in the composition 25P:75T as a consequence of the higher number of methyl groups in the PDMS chains. At the same time, the intensity of this peak is lower in the case of MTMS precursor, as this monomer has only one methyl group bonded to the silicon atom. 25D:75T and 4P:96T, with a similar number of dimethyl species, exhibit a peak intensity in the same range, as expected. The different precursor conditions the mobility of these methyl groups, as a sharp peak related to very mobile CH_3 units was detected for the 25P:75T network at 0.07 ppm. The other materials display a broader peak at 0.20 ppm, which is associated to methyl groups with restricted motions, fact that could be related to a more rigid crosslinked sol-gel structure [27]. Regarding the peak at 1.2 ppm, which is associated to the presence of isolated, water inaccessible, silanol groups [28], no differences were found among the materials 25M:75T, 25D:75T and 4P:96T. However, the signal considerably decreases when the amount of PDMS chains increases in the network. The ^{1}H NMR signal associated to hydrogen bonded silanol groups is higher in the composition with DMDES (peak at 3.3 ppm) [28]. The position of this signal is slightly shifted to higher values depending on the composition. This peak displacement can be related to distinct organic and inorganic population distributions in the sol-gel networks, so the silanol shift depends on their proximity to the methyl units. It is also detected a shoulder around 3.9 – 4.1 ppm, which is related to the presence of physisorbed water in the siloxane structure [27]. In addition, 25M:75T, 25D:75T and 4P:96T networks could contain free water in their structure (shoulder at 5.6 ppm) [28]. For the material 25P:75T, the amount of physisorbed water interacting in the network is lower with

respect to the other compositions and no free water-related signal was detected, probably due to its higher content of methyl groups.

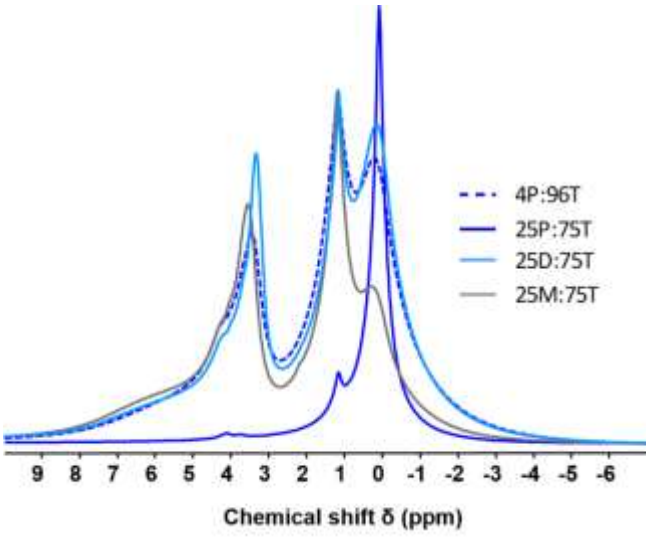

Figure 2. ^{1}H MAS NMR spectra for the hybrid networks synthetized using different precursors.

The ^{29}Si MAS NMR spectra are displayed in Figure 3 and the quantitative analysis obtained by fitting these results is shown in Table 2.

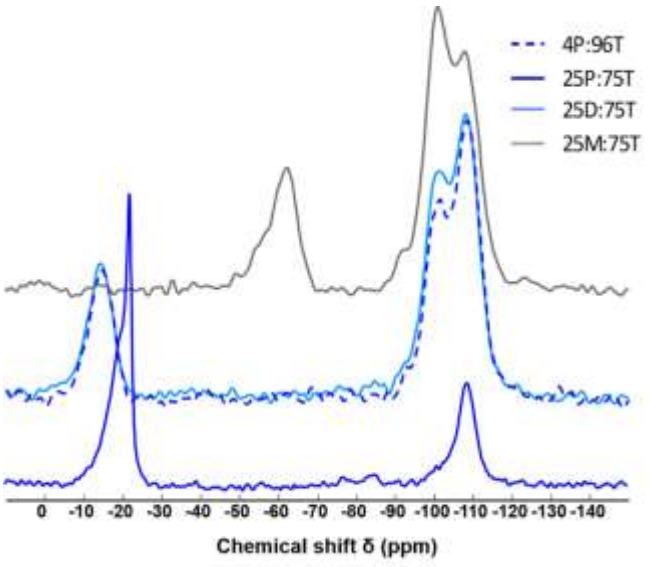

Figure 3. ^{29}Si MAS NMR (b) spectra for the hybrid networks synthetized using different precursors.

Three distinct groups of structural units related to the Si atom are detected. The first group of signals with chemical shift values between -12 and -23 ppm is associated to dimethylsiloxane D structural units ($(CH_3)_2{\cdot}SiO_2$). The second group is assigned to the trifunctional silicon (T units - $CH_3{\cdot}SiO_3$) and their signals are comprised between shifts of - 57 and - 62 ppm. The chemical shifts between -80 to -110 ppm are related to tetrafunctional Q structural units (SiO_4) [29].

Regarding the signals in the D region, D_a signal at -12 ppm is detected in the 4P:96T sample and can be associated to D groups linked to hydroxyls [30]. This signal is not detected in the sample with more PDMS, fact that is coherent with the low intensity of the ^{1}H NMR peak related to the presence of silanol groups. The signals D_b and D_c, between -14 and -20.3 ppm, can be attributed to D_2 units, which are bonded to Q units. In the PDMS-based networks, the deviation of these chemical shifts from the -23 ppm value associated to the pure PDMS is due to the nature of the first, and even the second neighbouring atom [30]. The sharp peak at -22.2 ppm in the 25P:75T spectrum corresponds to long PDMS chains [29]. T^3 signal at -62.5 ppm and T^2 at -57.1 ppm are obtained with the MTMS based sample [24]. Signals at around -93, -100 and -108 ppm supposes the formation of Q^2, Q^3 and Q^4 structures, respectively, probably linked to hydroxyl groups [28]. In general, a high degree of TEOS crosslinking is achieved with its combination with the three distinct precursors, as no Q^0 and Q^1 signals were found. The 75P:25T material is the most condensed network and only Q^4 signal was detected in its spectrum. This crosslinking level decreased with the reduction of the PDMS amount. The 4P:96T material displayed a spectrum that is similar to the one of the material synthetized using DMDES, being in both cases Q^4 the most intense peak. Nevertheless, the ratio Q^4/Q^3 for the DMDES network was slightly lower. The use of MTMS precursor clearly resulted in the less condensed structure as Q^3 became more intense than Q^4 and the Q^2 signal was identified.

Table 2. Chemical Shift δ and relative intensity (% I) of the identified structural units in the ^{29}Si MAS NMR spectra fitting.

Structural units	25M:75T		25D:75T		4P:96T		25P:75T	
	δ (ppm)	% I	δ (ppm)	% I	δ (ppm)	% I	δ (ppm)	% I
D_a	-	-	-	-	-12,0	8,6	-	-
D_b	-	-	-14,1	21,4	-15,2	14,3	-17,9	27,2
D_c	-	-	-	-	-	-	-20,6	21,1
D_d	-	-	-	-	-	-	-22,2	11,8
T^2	-57,1	9,7	-	-	-	-	-	-
T^3	-62,5	12,4	-	-	-	-	-	-
Q^2	-92,7	4,3	-	-	-	-	-	-
Q^3	-100,4	32,2	-100,5	38,3	-100,5	31,4	-102,7	11,6
Q^4	-108,1	41,4	-108,7	40,4	-108,7	45,7	-108,9	24,0

3.3. Coating adhesion and morphology characterization

The 25M:75T, 25D:75T and 25P:75T developed coatings were homogenous, transparent and well bonded to the substrates. The 4P:96T material, synthetized as control, was not suitable to be used as coating onto the stainless steel due to the high amount of TEOS in its composition. However, as previously explained in point 2.1, this composition was designed only as control for the structural and chemical evaluation. The coating-metal adhesion was evaluated through the cross-cut test and the coatings obtained with the three distinct methyl-modified alkoxysilanes achieved the maximum degree of adherence. Figure 4a shows the measured coating thicknesses. 25M:75T and 25P:75T materials had similar thickness, without statistical differences; while the 25D:75T coating was significantly thinner. The 25M:75T and 25D:75T deposited films showed similar Ra values with a roughness decrease with respect to the stainless steel (Figure 4b). However, the 25P:75T coating displayed a significant higher roughness in comparison with the substrate, the 25M:75T and the 25D:75T.

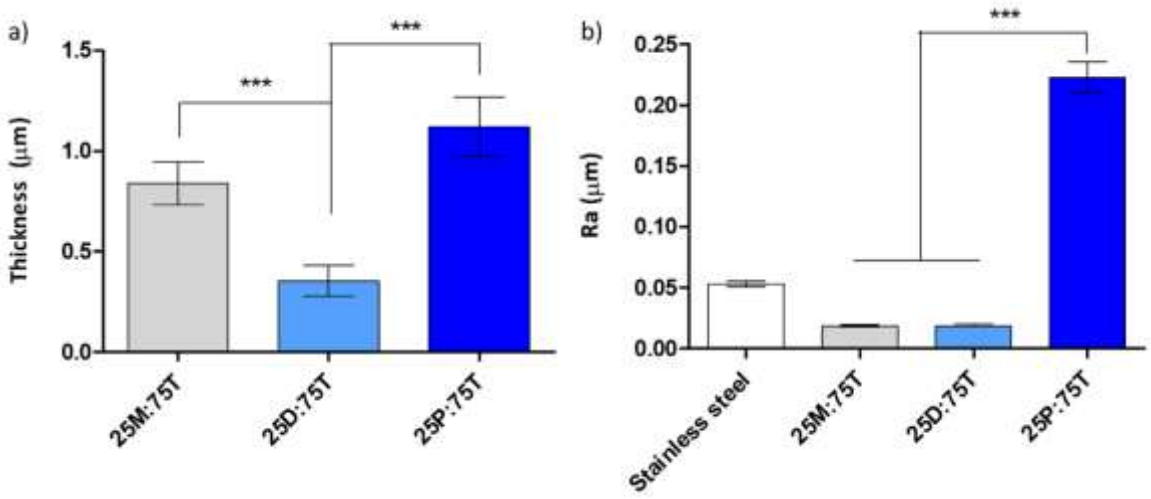

Figure 4. Coating thickness (a) and roughness (b) results. Bars indicate standard deviations. Statistical analysis was performed using one-way ANOVA with a Kruskal-Wallis post-hoctest (***, $p < 0.001$).

3.4. Contact angle

Contact angle measurements were carried out in order to evaluate the wettability of the distinct formulations (Figure 5).

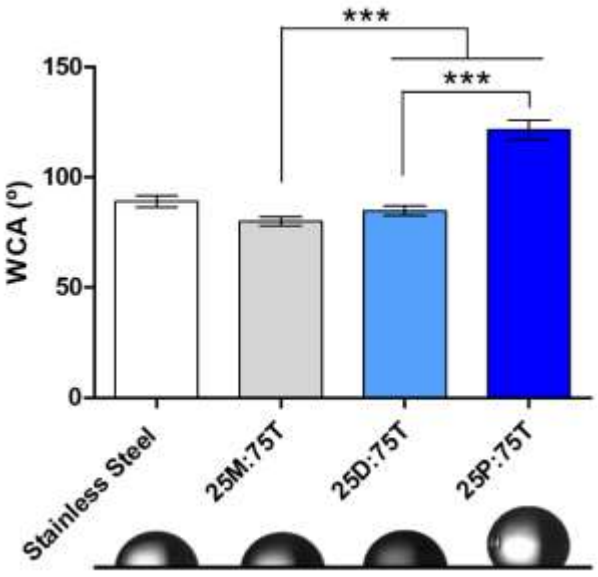

Figure 5. Contact angle results for 25M:75T, 25D:75T and 25P:75T hybrid sol-gel films deposited on stainless steel substrates. Bars indicate standard deviations. Statistical analysis was performed using one-way ANOVA with a Kruskal-Wallis post-hoctest (***, $p < 0.001$).

Results show that both stainless steel and 25D:75T surfaces displayed no statistical differences in wettability, being the measured contact angles onto their surfaces 89.07 ± 2.50º and 84.75 ± 2.14º, respectively. The 25M:75T coating presented the most hydrophilic character with a contact angles of 84.75 ± 2.05 º, whereas the coating with PDMS, the hybrid network with more methyl units, showed an hydrophobic character with 121,42 ± 4,42 º contact angle values.

3.5. Hydrolytic degradation

The results of mass loss as a function of immersion time are depicted in Figure 6 from which the kinetics of degradation of the three different coatings can be assessed. It is observed that the sol-gel network degradation is dependent on the employed precursor. 25P:75T and 25M:75T coatings, despite their distinct organic load, surprisingly display similar degradation rates. Both materials exhibit a high mass loss during the first week (≈14%), and after that their degradation rates become moderate reaching values of approximately 16 % for 25P:75T and 19 % for 25M:75T after 86 days in distilled water. The DMDES-coating shows a significant lower degradation kinetic with respect to the other compositions. A mass loss of ≈7 % during the first 52 days of incubation is observed and then its degradation increases until ≈13 % after 86 days of essay.

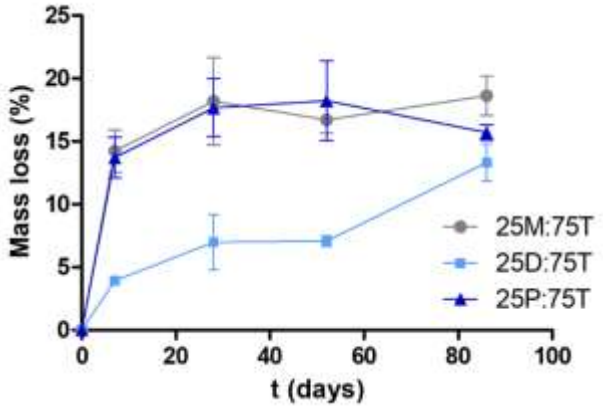

Figure 6. Mass loss kinetics during the hydrolytic degradation for hybrid sol-gel coatings synthetized using different methyl-modified alkoxysilanes as precursors. Bars indicate standard deviations.

3.6. Electrochemical Impedance Spectroscopy tests

25M:75T, 25D:75T and 25P:75T materials were applied as coatings onto stainless steel plates to perform the EIS tests. The results at 1.5 h and 48 h are shown in Figure 7. Different electrochemical behaviours were detected depending on the precursor used in the coating system. In this sense, a greater modulus of impedance (IZI) was observed for the material with PDMS, which in turn supposed a greater phase angle (θ) in all frequencies. Figure 7b and 7d show how the phase angle value drop occurs at a higher frequency in 25M:75T than in 25D:75T coating, being the 25P:75T material the coating that maintained the angle at - 90 º in a wider frequency range. This trend suggests a capacitive behaviour, showing that the PDMS-based sol-gel was the coating with the higher protection capability. In contrast, the material synthesized from MTMS showed a lower resistance against corrosion.

A decrease in the coating protective capabilities was detected over time in all materials, although the spectra shapes are maintained. Thus, comparing the results at 1.5 and 48 h, the three coatings

displayed a slight reduction of impedance modulus and a smaller frequency range with high values of phase angles at high frequencies.

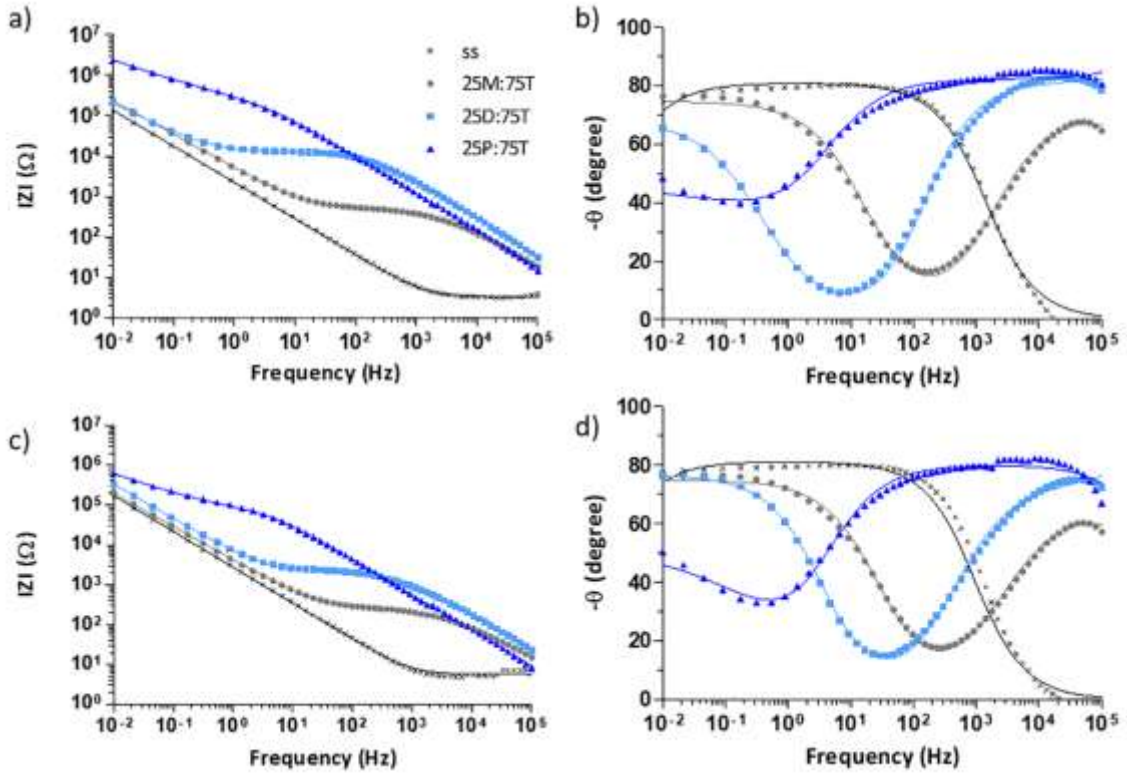

Figure 7. EIS bode plots: impedance modules (a and c) and phase angle (b and d) for stainless steel, 25M:75T, 25D:75T and 25P:75T coatings after 1.5 h (a and b) and 48 h (c and d) of immersion in the electrolyte. Fitted results are represented by the solid lines.

The measured spectra were fitted to equivalent circuits using Z-view software. For the bare stainless steel only the natural formation of the oxide layer in the steel was observed. However, sol-gel coated stainless steel samples presented two distinct processes, the first one related to the coating at high frequencies and the other, at low frequencies, related to the characteristic substrate oxide layer.

An equivalent circuit of one time constant was employed for the control sample, the stainless steel substrate (Figure 8a); while a model with two time constants was used to fit the coated sample results (Figure 8b). This kind of equivalent circuits are widely used to model EIS spectra [9,31]. In Figure 8a, Rs is the electrolyte resistence, Rox and CPEox correspond to the oxide layer resistance and Constant Phase Element, respectively. At the same time, in Figure 8b, the coating signal is added using Rcoat and CPEcoat. These both parameters can be related to the barrier properties of the sol-gel networks and their capability to protect the substrate. Rcoat is associated to the porosity and the coating degradation, while CPEcoat can be linked to the water absorption in the sol-gel.

Contact Phase Elements (CPE) had to be employed in the models instead of the capacitance elements (Cc). For this reason, CPE values are displayed in $s^n\Omega^{-1}$ units, being n an exponent which is obtained in the fitting. n parameter can comprise values between 0 and 1 and is associated to a non-uniform current distribution on the tested surface as consequence of roughness or other distributed properties. Known the value of n, the capacitances can be calculated in F units. Cc is directly related to the material permeability to water penetration through the Equation 1, then greater values of Cc can be correlated to an increased permittivity.

$$Cc = \varepsilon\varepsilon_0 A/d\,, \tag{1}$$

where ε is the dielectric constant of the material, ε_0 is the vacuum permittivity, A is the coating area in contact with the electrolyte and d, the thickness.

The resulted fittings were quite good with high correlation in all cases (Chi-squared<0.01), as can be observed in Figure 7. It should be mentioned that in the coated systems the electrochemical parameters referred to the stainless steel oxide layer properties are not well defined in the normal measuring frequency range. Anyway, the objective of this characterization is to evaluate the sol-gel

coating properties related to the parameters Rcoat and CPEcoat, which are displayed in Figure 8c and 8d.

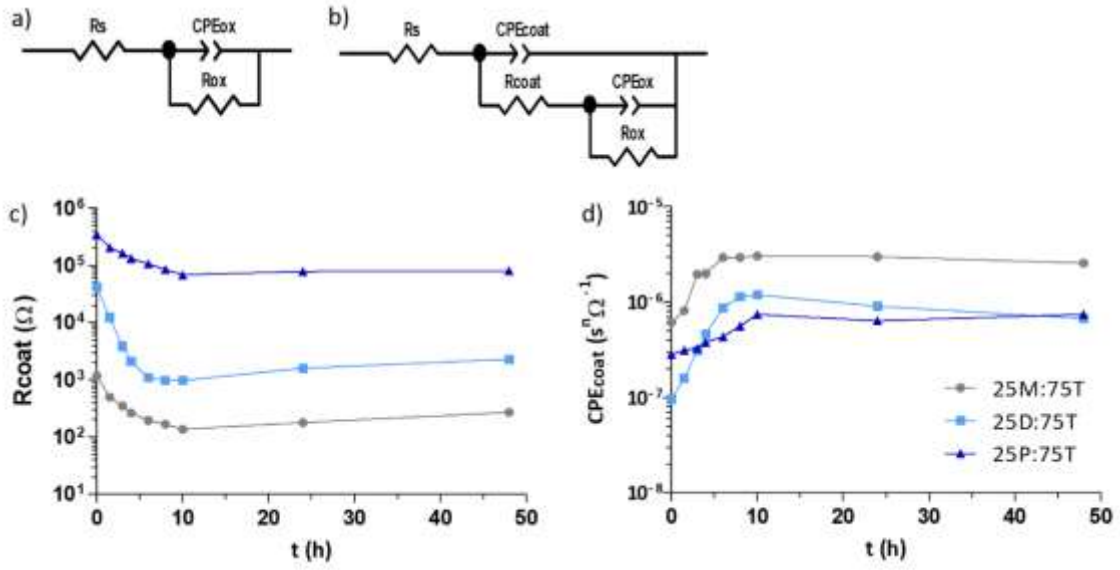

Figure 8. Equivalent circuits used for (a) non-coated and (b) sol-gel coated samples. Rcoat (c) and CPEcoat (d) versus time of contact with electrolyte (3.5 % wt. NaCl) for 25M:75T, 25D:75T and 25P:75T sol-gel coatings.

Figure 8c shows how the Rcoat value decreases with the time of contact with the saline solution in all samples. This reduction of Rcoat is higher during the first 6 h and then the systems display a steady resistance, even detecting a slight increase at 48 h, likely attributed to the formation of deposits from the solution, which would clog the coating pores [31]. Regarding the effect of the precursor selection, the network with PDMS presented higher values of Rcoat from the first moment of contact with the electrolyte, while the coating with MTMS displayed the poorest barrier protection capability.

CPE elements were used instead of capacitances and the values of the parameter n are shown in Table 3. This parameter is related to the corrosion mechanisms and acquires the value 1 for pure

capacitors, 0 for resistors and 0.5 when the corrosion mechanism is dominated by a semi-infinite length diffusion phenomena. The tested coatings exhibited n values in the range 0.74-0.94, which are closer to those ascribed to capacitive behaviours.

Table 3. Values of parameter n related to CPEcoat elements for each coating and measuring time.

Coating	0 h	1.5 h	3 h	4 h	6 h	8 h	10 h	24 h	48 h
25M:75T	0,84	0,83	0,76	0,77	0,74	0,75	0,75	0,75	0,76
25D:75T	0,94	0,91	0,86	0,84	0,80	0,78	0,77	0,80	0,82
25P:75T	0,90	0,90	0,91	0,90	0,89	0,86	0,85	0,91	0,89

In Figure 8d, it can be seen how the CPE value increased with the time of contact with the electrolyte in the three sol-gel coatings. This increase of CPE is more severe during the first stage of immersion, possibly due to the initial adsorption of water in the sol-gel network. Additionally, it is the MTMS-based coating that displayed the highest CPE values, whereas the sol-gel networks synthetized using PDMS and DMDS showed lower values of CPE and higher n parameters, proving their highest barrier properties against corrosion. On the other hand, although the coating 25D:75T showed lower CPE values than the 25P:75T at the beginning of the essay, the DMDES coating CPEs increased above those of the PDMS with the immersion time. So, the 25P:75T showed a greater stability.

4. Discussion

The sol-gel hybrid materials obtained from alkoxysilanes have great potential to be employed in biomedical applications, especially those associated to bone system [7]. These materials can be applied as coatings, acting as metallic prosthesis/implant protection against the biological environment corrosion. At the same time, these materials can bioactivate the metal surface, giving these devices the ability to promote bone regeneration, either by their intrinsic orthosilicic acid release or by the use of the sol-gel material as a vehicle of release of compounds with osteogenic

properties [32]. However, these two effects (protection and bioactivation) are opposed. As more degradable is the sol-gel network, greater is the reached bioactivation; but in turn, it will have poorer corrosion protective properties. For this reason, it is essential to be able to design sol-gel structures with an adequate balance between protection and bioactivation for each specific application. Thus, understanding the precursor selection effect on the final sol-gel coatings properties is vital for obtaining the required features. Within this context, the aim of this study was to evaluate the feasibility of using three distinct methyl-modified alkoxysilanes (MTMS, DMDES and PDMS) as precursors to develop sol-gel coatings for biomedical applications.

The chemical characterization of these hybrid materials allowed to confirm the suitability of the employed synthesis route, as the sol-gel reactions were carried out correctly, leading to networks with high condensation degrees. The ^{29}Si-NMR clearly showed how the less condensed structure was obtained with the MTMS precursor (Figure 3). In addition, both ^{1}H-NMR and FT-IR results established that in all cases the methyl groups associated to the evaluated alkoxysilanes are present in the structures of the developed materials. These results also allowed to assess the different amounts of methyl groups in the networks depending on the employed precursors. Then, the material with PDMS displayed the most intense signals associated to this chemical group, while the material with MTMS had a more inorganic character with less $–CH_3$ groups in its structure (Figure 2). The ^{1}H-NMR also revealed differences in the CH_3 mobility in the distinct developed sol-gel networks. The DMDES and MTMS networks should have more rigid structures than the PDMS-based material. These hybrid networks not only displayed distinct degrees of crosslinking and mobility, but also showed, by ^{1}H-NMR analysis, dissimilar distribution of the organic and inorganic population into the structure. The greater proximity between the organic moieties and the silanol groups in the DMDES- and MTMS-based hybrids could suggest a closer mixture of both organic and inorganic

populations, whereas the separation of these populations should be higher in the composition with PDMS.

The three precursors allowed to obtain coatings onto the stainless steel with a suitable adhesion of the material onto this substrate for the ratio precursor:TEOS 1:3 . However, differences among the distinct coatings were found in surface parameters as roughness and wettability. These parameters are key to achieve a proper interaction of the biomaterial with the biological environment and, consequently, achieve a good performance [33]. Regarding the wettability, contact angle values below 90º are associated with hydrophilic behaviour, while for angles above 90º the surface is considered hydrophobic. Rupp *et al.* [34] reported that hydrophilic surfaces can facilitate the initial biomaterial-bone tissue interactions, favouring wound healing and osseointegration. As can be seen in Figure 5, both 25M:75T and 25D:75T showed contact angle values characteristic of hydrophilic surfaces. However, the coating with PDMS displayed a strong hydrophobic character with a contact angle of around 121 º. These values can be directly related to the major or minor organic character of the composition [9]. So, as more methyl groups are present in the hybrid, more hydrophobic is the resulting coating. On the other hand, the MTMS and DMDES networks gave rise to a coating smoother than the PDMS material. The PDMS-based coating displayed a significantly higher surface roughness (Figure 4b). These differences can play a pivotal role on the protein adsorption onto the biomaterial and therefore, condition the success of the biomaterial [35,36]. *In vitro* studies suggest that there is a positive effect of surface roughness on osteoblast cell activity, which can indicate the achievement *in vivo* of greater bone fixation degrees with rough surfaces [37].

The hydrolytic degradation of these materials was associated to the release of Si compounds, which are able to bioactivate the bone tissue healing process around implants [11]. As can be seen in Figure 6, the MTMS-coating was the most degraded coating, fact that could be related to its greater inorganic nature and less condensed structure. The coating with PDMS, which has a higher amount

of methyl functional groups, showed a degradation rate similar to that of 25M:75T, whereas the coating with DMDES displayed the slowest degradation kinetics. This behaviour could be explained by the distinct distribution of organic and inorganic populations into the network detected by ^{1}H-NMR. So, the PDMS:TEOS structure could result weaker against the hydrolytic attack due to the likely higher separation between the organic and inorganic species into its network. On the other hand, the network with DMDES reaches a greater mixture of inorganic and organic moieties, thus becoming more difficult to be degraded. In this case, the low chemical affinity between methyl groups and water could better protect the material. Nevertheless, at the end, all coatings showed moderate differences in the total network mass loss after 86 days.

Regarding the capability of these coatings to protect metallic implants against corrosion, Rcoat and CPEcoat parameters (Figure 8) showed as the material protective properties are reduced when the MTMS precursor is employed. The more hydrophilic and inorganic character, with the less condensated structure, of the MTMS resulting coating would facilitate the water adsorption into its network and its degradation by hydrolysis. Moreover, this fact is in agreement with its higher degradation rate seen from the hydrolytic degradation results. Otherwise, the material with PDMS displayed the most capacitive and barrier behaviour in EIS results. This fact can be attributed to its high hydrophobicity and the major amount of $–CH_3$ units in its structure, which would make water penetration into the network more difficult. However, these initial highest protective properties could vanish at longer times, as the hydrolytic degradation of this network showed a degradation rate similar to the one of the coating with MTMS. Despite its slower degradation, the DMDES-based coating displayed an intermediate capacity of the metallic substrate protection with respect to the PDMS and MTMS electrochemical results. This fact could be associated to the lesser thickness of this coating (Figure 4a). Surprisingly, this coating even having less thickness and lower organic

functional groups in their structure showed CPEcoat values similar to those of the PDMS-based composition.

Finally, having into account all the results obtained, the sol-gel material synthetized from MTMS could be considered the more degradable network and, therefore, it could become the most bioactive by its higher ability to release Si. On the other hand, the precursors PDMS and DMDES gave rise to coatings with higher protective capability against corrosion. Interestingly, the more cohesive network obtained from the DMDES precursor, together with its more dilatory degradation kinetics, could suggest the use of this precursor to develop hybrid sol-gel release vehicles when longer delivery times are required. Otherwise, the coating with MTMS could result useful for releasing compounds in shorter times. Confidently, in a next step, the *in vitro* biological evaluation of these three compositions will shed more light on their capabilities as biomaterials and on their performance as coatings on biomedical metals.

5. Conclusions

In this study, we have developed three different hybrid sol-gel compositions from the combination of three distinct methyl-modified alkoxysilanes (MTMS, DMDES and PDMS) and TEOS to be applied as coatings onto AISI 316-L stainless steel. In all cases, it was possible to obtain homogeneous and well-adhered coatings onto this metallic substrate. Depending on the used precursor, the designed coatings displayed different protective capabilities against corrosion and kinetic degradations by hydrolysis. The material with MTMS showed the highest ability to release Si compounds, whereas the PDMS- and DMDES-based coatings displayed greater protective properties. Moreover, the chemical structure obtained using this DMDES as precursor suggested the potential interest of this material as vehicle release. As a next step in this work, the assessment of biological assays will be very important to confirm the suitability of these formulations as biomaterials.

Acknowledgments

This work was supported by MINECO [MAT MAT2017-86043-R], Universitat Jaume I under [UJI-B2017-37; Predoc/2014/25; and the researcher mobility grant E-2016-31], University of the Basque Country under [UFI11/56] and Basque Government under [IT611-13]. In addition, this work was developed within the scope of the project CICECO-Aveiro Institute of Materials, FCT Ref. [UID/CTM/50011/2019], financed by national funds through the FCT/MCTES. The NMR spectrometers used in this work are part of the Portuguese National NMR Network (PTNMR) and are partially supported by Infrastructure Project Nº 022161 (co-financed by FEDER through COMPETE 2020, POCI and PORL and FCT through PIDDAC). Authors would like to thank Raquel Oliver and Jose Ortega for their valuable technical assistance.

REFERENCES

[1] L.L. Hench, The story of Bioglass®, J. Mater. Sci. Mater. Med. 17 (2006) 967–978. doi:10.1007/s10856-006-0432-z.

[2] J.R. Jones, Reprint of : Review of bioactive glass : From Hench to hybrids, Acta Biomater. 23 (2015) S53–S82. doi:10.1016/j.actbio.2015.07.019.

[3] C.J. Brinker, G.W. Scherer, Sol-gel Science - The Physics and Chemistry of Sol-gel Processing, Elsevier Academic Press, San Diego, 1990.

[4] H. Schmidt, H. Scholze, A. Kaiser, Principles of hydrolysis and condensation reaction of alkoxysilanes, J. Non. Cryst. Solids. 63 (1984) 1–11. doi:10.1016/0022-3093(84)90381-8.

[5] E.M. Carlisle, Silicon: A requirement in bone formation independent of vitamin D1, Calcif. Tissue Int. 33 (1981) 27–34. doi:10.1007/BF02409409.

[6] D.M. Reffitt, N. Ogston, R. Jugdaohsingh, H.F.J. Cheung, B.A.J. Evans, R.P.H. Thompson, J.J. Powell, G.N. Hampson, Orthosilicic acid stimulates collagen type 1 synthesis and osteoblastic differentiation in human osteoblast-like cells in vitro, Bone. 32 (2003) 127–135. doi:10.1016/S8756-3282(02)00950-X.

[7] M. Vallet-Regí, M. Colilla, B. González, Medical applications of organic-inorganic hybrid materials within the field of silica-based bioceramics, Chem. Soc. Rev. 40 (2011) 596–607. doi:10.1039/c0cs00025f.

[8] R.M. Pilliar, Sol–gel surface modification of biomaterials, in: C. Wen (Ed.), Surf. Coat. Modif. Met. Biomater., Elsevier, 2015: pp. 185–217. doi:10.1016/B978-1-78242-303-4.00006-5.

[9] F. Romero-Gavilán, S. Barros-Silva, J. García-Cañadas, B. Palla, R. Izquierdo, M. Gurruchaga, I. Goñi, J. Suay, Control of the degradation of silica sol-gel hybrid coatings for metal implants prepared by the triple combination of alkoxysilanes, J. Non. Cryst. Solids. 453 (2016) 66–73. doi:10.1016/j.jnoncrysol.2016.09.026.

[10] A. Mombelli, D. Hashim, N. Cionca, What is the impact of titanium particles and biocorrosion on implant survival and complications ? A critical review, Clin. Oral Implants Res. 29 (2018) 37–53. doi:10.1111/clr.13305.

[11] M. Martínez-Ibáñez, M.J. Juan-Díaz, I. Lara-Saez, A. Coso, J. Franco, M. Gurruchaga, J. Suay Antón, I. Goñi, Biological characterization of a new silicon based coating developed for dental implants., J. Mater. Sci. Mater. Med. 27 (2016) 80. doi:10.1007/s10856-016-5690-9.

[12] A. Borówka, Effects of twin methyl groups insertion on the structure of templated mesoporous silica materials, Ceram. Int. 45 (2019) 4631–4636. doi:10.1016/j.ceramint.2018.11.152.

[13] Q. Wang, Fang; Liu, Jianhong; Luo, Zhongkuan; Zhang, J. Wang, Peixin; Liang, Xun; Li, Cuihua; Chen, Effects of dimethyldiethoxysilane addition on the sol–gel process of tetraethylorthosilicate, J. Non. Cryst. Solids. 353 (2007) 321–326.

[14] H. Zhang, X. Hu, Y. Sun, Y. Zheng, L. Yan, B. Jiang, H. Chen, X. Zhang, Design and sol-gel preparation of a six-layer tri-wavelength ORMOSIL antireflective coating for a high power laser system, RSC Adv. 6 (2016) 31769–31774. doi:10.1039/c6ra04584g.

[15] K.H. Lee, S.H. Rhee, The mechanical properties and bioactivity of poly(methyl methacrylate)/SiO2-CaO nanocomposite, Biomaterials. 30 (2009) 3444–3449. doi:10.1016/j.biomaterials.2009.03.002.

[16] P. Kortesuo, M. Ahola, M. Kangas, T. Leino, S. Laakso, L. Vuorilehto, A. Yli-Urpo, J. Kiesvaara, M. Marvola, Alkyl-substituted silica gel as a carrier in the controlled release of dexmedetomidine, J. Control. Release. 76 (2001) 227–238. doi:10.1016/S0168-3659(01)00428-X.

[17] A.G.B. Castro, A.C. Bastos, V. Galstyan, G. Faglia, G. Sberveglieri, I.M. Miranda Salvado, Synthesis and electrochemical study of a hybrid structure based on PDMS-TEOS and titania nanotubes for biomedical applications, Nanotechnology. 25 (2014). doi:10.1088/0957-4484/25/36/365701.

[18] K.M.F. Rossi de Aguiar, M. V. Nascimento, J.L. Faccioni, P.L.M. Noeske, L. Gätjen, K. Rischka, U.P. Rodrigues-Filho, Urethanes PDMS-based: Functional hybrid coatings for metallic dental implants, Appl. Surf. Sci. 484 (2019) 1128–1140. doi:10.1016/j.apsusc.2019.04.058.

[19] P.A. Tran, K. Fox, N. Tran, Novel hierarchical tantalum oxide-PDMS hybrid coating for medical implants: One pot synthesis, characterization and modulation of fibroblast proliferation, J. Colloid Interface Sci. 485 (2017) 106–115. doi:10.1016/j.jcis.2016.06.048.

[20] S. Tavakoli, S. Nemati, M. Kharaziha, S. Akbari-Alavijeh, Embedding CuO Nanoparticles in PDMS-SiO2 Coating to Improve Antibacterial Characteristic and Corrosion Resistance, Colloids Interface Sci. Commun. 28 (2019) 20–28. doi:10.1016/j.colcom.2018.11.002.

[21] F. Rubio, J. Rubio, J.L. Oteo, A FT-IR Study of the Hydrolysis of Tetraethylorthosilicate (TEOS)., Spectrosc. Lett. 31 (1998) 199–219. doi:10.1080/00387019808006772.

[22] J.C. Almeida, A.G.B. Castro, I.M. Miranda, F.M.A. Margaça, M.H. Vaz, A new approach to the preparation of PDMS – SiO 2 based hybrids – A structural study, Mater. Lett. 128 (2014) 105–109. doi:10.1016/j.matlet.2014.04.135.

[23] J.C. Almeida, A.G.B. Castro, J.J.H. Lancastre, I.M. Miranda Salvado, F.M.A. Margaça, M.H.V. Fernandes, L.M. Ferreira, M.H. Casimiro, Structural characterization of PDMS–TEOS–CaO–TiO2 hybrid materials obtained by sol–gel, Mater. Chem. Phys. 143 (2014) 557–563. doi:10.1016/j.matchemphys.2013.09.032.

[24] M.J. Juan-Díaz, M. Martínez-Ibáñez, M. Hernández-Escolano, L. Cabedo, R. Izquierdo, J. Suay, M. Gurruchaga, I. Goñi, Study of the degradation of hybrid sol–gel coatings in aqueous medium, Prog. Org. Coatings. 77 (2014) 1799–1806. doi:10.1016/j.porgcoat.2014.06.004.

[25] L. Téllez, J. Rubio, F. Rubio, E. Morales, J.L. Oteo, No TFT-IR Study of the Hydrolysis and Polymerization of Tetraethyl Orthosilicate and Polydimethyl Siloxane in the Presence of Tetrabutyl Orthotitanateitle, Spectrosc. Lett. 37 (2004) 11–31. doi:10.1081/SL-120028420.

[26] J.C. Almeida, A. Wacha, A. Botá, L. Almásy, M.H. Vaz Fernandes, F.M.A. Margaça, I.M. Miranda Salvado, PDMS-SiO2 hybrid materials e A new insight into the role of Ti and Zr as additives, Polymer (Guildf). 72 (2015) 40–51. doi:10.1016/j.polymer.2015.06.053.

[27] J. Brus, Solid-state NMR study of phase separation and order of water molecules and silanol groups in polysiloxane networks, J. Sol-Gel Sci. Technol. 25 (2002) 17–28. doi:Doi 10.1023/A:1016032809131.

[28] H.N. Kim, S.K. Lee, Atomic structure and dehydration mechanism of amorphous silica: Insights from 29Si and 1H solid-state MAS NMR study of SiO2 nanoparticles, Geochim. Cosmochim. Acta. 120 (2013) 39–64. doi:10.1016/j.gca.2013.05.047.

[29] F. Babonneau, Hybrid siloxane-oxide materials via sol-gel processing: Structural characterization, Polyhedron. 13 (1994) 1123–1130. doi:10.1016/S0277-5387(00)80249-1.

[30] J.C. Almeida, A. Wacha, P.S. Gomes, M.H.R. Fernandes, M.H. Vaz, I.M. Miranda, PDMS-SiO2-TiO2-CaO hybrid materials - Cytocompatibility and nanoscale surface features, Mater. Sci. Eng. C. 64 (2016) 74–86. doi:10.1016/j.msec.2016.03.071.

[31] A.A. EL Hadad, E. Peón, F.R. García-galván, V. Barranco, J. Parra, A. Jiménez-morales, J.C. Galván, Biocompatibility and Corrosion Protection Behaviour of Hydroxyapatite Sol-Gel-Derived Coatings on, Materials (Basel). 10 (2017) 94. doi:10.3390/ma10020094.

[32] G.J. Owens, R.K. Singh, F. Foroutan, M. Alqaysi, C. Han, C. Mahapatra, H. Kim, Sol – gel based materials for biomedical applications, Prog. Mater. Sci. 77 (2016) 1–79. doi:10.1016/j.pmatsci.2015.12.001.

[33] C. Nelson, Y. Oshida, J. Henrique, C. Lima, C. Alberto, Relationship between surface properties (roughness , wettability and morphology) of titanium and dental implant removal torque, J Mech Behav Biomed Mater. 1 (2008) 234–242. doi:10.1016/j.jmbbm.2007.12.002.

[34] F. Rupp, R.A. Gittens, L. Scheideler, A. Marmur, B.D. Boyan, Z. Schwartz, J. Geis-gerstorfer, Acta Biomaterialia A review on the wettability of dental implant surfaces I : Theoretical and experimental aspects, Acta Biomater. 10 (2014) 2894–2906.

doi:10.1016/j.actbio.2014.02.040.

[35] F. Romero-Gavilán, A.M. Sanchez-Pérez, N. Araújo-Gomes, M. Azkargorta, I. Iloro, F. Elortza, M. Gurruchaga, I. Goñi, J. Suay, Proteomic analysis of silica hybrid sol-gel coatings: a potential tool for predicting the biocompatibility of implants in vivo, Biofouling. 33 (2017) 676–689. doi:10.1080/08927014.2017.1356289.

[36] F. Romero-Gavilán, N.C. Gomes, J. Ródenas, A. Sánchez, F. , Mikel Azkargorta, Ibon Iloro, I.G.A. Elortza, M. Gurruchaga, I. Goñi, and J. Suay, Proteome analysis of human serum proteins adsorbed onto different titanium surfaces used in dental implants, Biofouling. 33 (2017) 98–111. doi:10.1080/08927014.2016.1259414.

[37] D. Buser, R.K. Schenk, S. Steinemann, J.P. Fiorellini, C.H. Fox, H. Stich, Influence of surface characteristics on bone integration of titanium implants. A histomorphometric study in miniature pigs, J. Biomed. Mater. Res. 25 (1991) 889–902. doi:doi.org/10.1002/jbm.820250708.